ARMA 22–0019

Approaches to Determine Fault Shear Strength in Large-scale Direct Shear Test Simulations using Discrete Fracture Networks

Kim, B.H. and Larson, M.K.
CDC/NIOSH, Spokane, Washington, United States

ABSTRACT: In this study, 3DEC modeling in conjunction with the Discrete Fracture Networks (DFNs) technique was performed to better understand the behavior of shearing faults in a relatively large-scale direct shear test model. The DFNs explicitly generated two different geometries of the fault plane surface indicating the stepped or smooth waviness of the surface using probability distribution functions to generate orientation, fracture density (or frequency), and size of the discrete fractures. A 3-dimensional block model of hundreds of meters was constructed for the direct shear test using 3DEC modeling software. After the completion of the direct shear test simulations, a shear strength of the fault plane was estimated by back calculation. The DFNs with subhorizontal/vertical dip angles created an imbricate structure that resulted in a stepped geometry and strong shear response in the fault plane. Under direct shear, the fault plane needed to break the asperities or block before any frictional behavior was allowed or the fault plane would dilate significantly. This resulted in higher shear strength of the fault plane. On the other hand, the DFNs with oblique dip angles generated a relatively smooth surface of the fault plane. The smooth surface of the fault plane allowed deformation principally parallel to the fault plane, and only a few failures developed across the rock blocks in the model. Consequently, the 3DEC model explicitly replicated the complicated geometries of the fault plane using the two very contrasting DFNs and allowed researchers to investigate different shear behaviors of fault planes as a function of surface conditions.

1. INTRODUCTION

The highly anisotropic characteristics of coal seams that result from geologic structures when mining takes place, such as cleats, bedding, faults, and spatial redistribution of induced stress in coal pillars, cause many uncertainties that affect safety. Dynamic failure in coal mines, known as "bumps," is one of the most challenging and persistent engineering problems associated with coal mining in highly stressed conditions. These events occur when stresses in a coal pillar, used for support in underground workings, exceed the critical strength of the pillar, causing the pillar to rupture without warning. These events can be exceptionally violent, ejecting coal and rock with explosive force [*1, 2*].

These events occur suddenly and often without warning. As such, miners often do not have the opportunity to move to safety before an event. Although relatively rare, dynamic failure events resulted in worker injury up to and including fatality in 52% of reported cases occurring from 2000–2019. Moreover, the fatality rate is roughly ten times greater than that associated with roof falls, a leading cause of ground-control-related injuries in underground coal mines [*3*]. However, a continuous effort to better understand the dynamic failure mechanism in coal mines is still required to make further improvements in preventing bump-related fatalities in underground coal mining.

This paper is part of an effort by the National Institute for Occupational Safety and Health (NIOSH) to identify risk factors associated with bumps in highly stressed ground conditions. More specifically, this paper reports an exploratory effort with an unconventional approach using a numerical tool to try to better understand a possible scenario where bump risk might be increased—that is, a scenario involving a normal fault. The objective is to assess whether a numerical tool might be useful or practical in forecasting bump potential associated with a fault-slip for a typical structural geologic setting.

The risk associated with faults/fault zones and coal bumps has been acknowledged by several researchers in the literature. Mauck [*4*] and Peperakis [*5*] mention the risk of bumps with regard to the proximity of mining operations to faults. Some describe the role of faults in stress concentration [*5-9*], thus causing conditions with increased bump risk. Others specifically mention fault slip and the resulting release of energy associated with bumps [*5, 7-10*]. Iannacchione and Zelanko [*11*] mention the role of geologic structure, including displacement faults, to concentrate stress and control the caving and heaving characteristics of strata. The risk of bumps associated with faults is well established; however, the specific mechanisms that cause bumps may not be well understood. Faults, in general, are simulated as a single planar or nonplanar interface by numerical tools for safety or stability analyses of underground mining excavations. However, the real 3D structure of a fault is commonly very complex, with different branches that reactivate at different times. Furthermore, these branches are zones of nonzero thickness where material continuously undergoes damage even during interseismic periods [*12*].

Although faults are commonly simulated as a single planar or nonplanar interface for a safety or stability analysis in underground mining excavations, the real 3D structure of a fault is often very complex with different branches that reactivate at different times [*12*]. Surface roughness and aperture are the most important factors influencing both the mechanical and hydraulic behaviors of faults [*13, 14*]. In this study, 3DEC [*15*] modeling in conjunction with the Discrete Fracture Networks (DFNs) technique was performed to better understand the behavior of shearing faults in a relatively large-scale direct shear test model. The DFNs explicitly generated two different geometries of the fault plane surface, indicating stepped or smooth waviness of the surface. This was accomplished using probability functions to generate orientation, fracture density (or frequency), and size of the discrete fractures.

This paper describes common approaches for a fault-slip analysis by direct shear test simulation. A 3-dimensional block model of hundreds of meters was constructed for the direct shear test using 3DEC. After the completion of the direct shear test simulations, a shear strength of the fault plane was estimated by back calculation.

2. METHODS

A 3-dimensional block model of hundreds of meters with 500(W) × 250(H) × 50(L) m was constructed for the direct shear simulation in 3DEC for this study. To create a 3-dimensional synthetic fault surface, different combinations of dip angle sets are presented in this section. A relatively rough surface is created by the two DFNs sets that are realized by mean dip angles of 0° and 90° (Fig. 1a). A relatively smooth surface is generated by another two DFNs sets that are realized by mean dip angles of 30° and 60° (Fig. 1b).

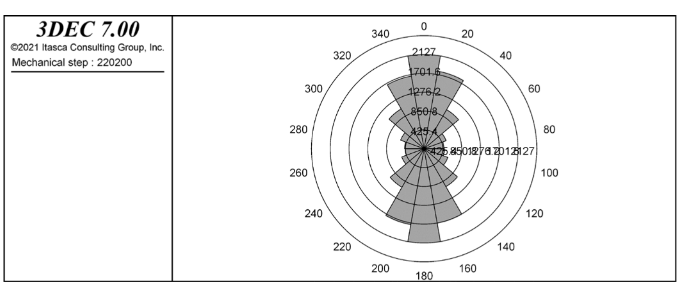

(a)

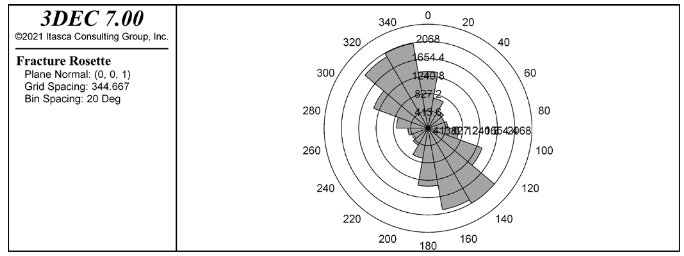

(b)

Fig. 1. DFNs Rosette plots (a) subhorizontal/-vertical sets for rough surface geometry; (b) oblique sets for rough surface geometry.

The Fisher distribution based on these orientations is used to generate the DFNs. The Power-law distribution is chosen to determine the sizes of the cleats (0.1 m ~ 10.0 m). The results of the DFNs realizations are shown in Fig. 2.

(a)

(b)

Fig. 2. Realized DFNs to simulate (a) rough synthetic fault surface by subhorizontal/vertical dip angles; (b) smooth synthetic fault surface by oblique dip angles.

The DFNs are created only in the aperture (i.e., fault) in the model. The heterogeneity of the engineering properties (i.e., cohesion and tensile strength) in the 3DEC models was also considered using Monte Carlo simulations. The heterogeneous strengths were modeled by populating the cohesion and tensile strengths of blocks and block contacts of the model using probability distributions. The built-in Mohr C++ plug-in [*16*] is used in the models. To create the numerical specimens, each block contact with the DFNs is assigned a cohesion and a tensile strength value randomly selected from the probability distributions generated by the Monte Carlo simulation as shown in Fig. 3. The range of the cohesion and the tensile strength is 2.7±1.8 MPa and 0.28±0.19 MPa, respectively. All subcontacts forming each contact are assigned the same tensile strength and cohesion. The realized properties in the 3DEC model is presented in Fig. 4. Assigned DFNs contacts cohesion by the Monte Carlo simulationTable 1 presents the input parameters used for the direct shear simulations in 3DEC.

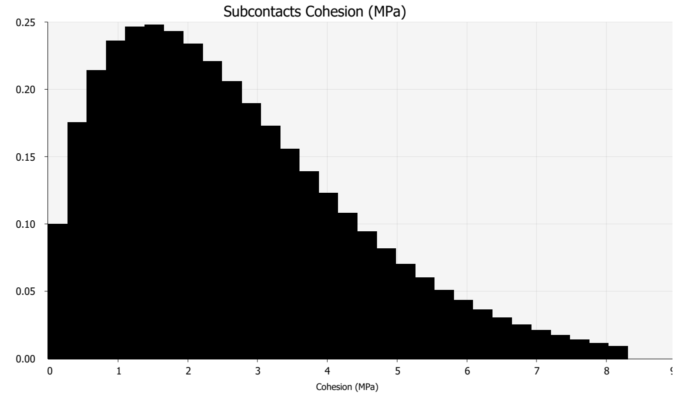

(a)

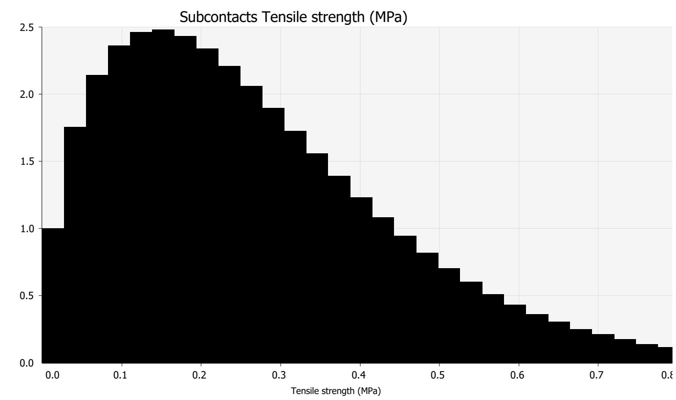

(b)

Fig. 3 The probability distributions generated by the Monte Carlo simulation for (a) cohesion and (b) tensile strength.

Table 1. Input data for the blocks and DFNs in the 3DEC model

Input parameter	Value
Unit weight (MN/m^3)	0.027
Block Young's modulus (GPa)	50
Block Poisson's ratio	0.2
DFNs normal stiffness (GPa/m/m)	305
DFNs shear stiffness (GPa/m/m)	120

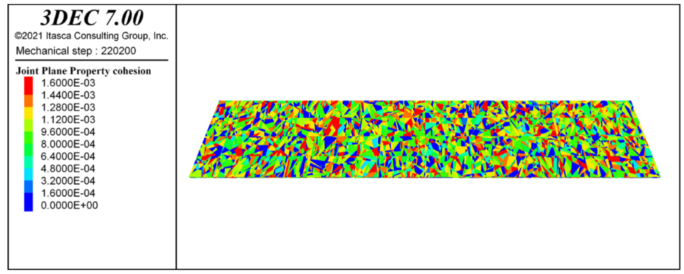

Fig. 4. Assigned DFNs contacts cohesion by the Monte Carlo simulation

All blocks in the 3DEC model were built as deformable and elastic blocks. The 3DEC models were used to calculate shear and normal displacements and stresses under constant normal stiffness conditions (CNS). Fig. 5 illustrates the layout of the 3DEC model for the direct shear test simulation. The red layer embedding the DFNs for the synthetic fault surface are created between the two rock blocks (blue and green). For the boundary condition, the bottom of the model is fixed in all directions, but the one-directional velocity vectors (red arrows) are applied on the right side of the top block.

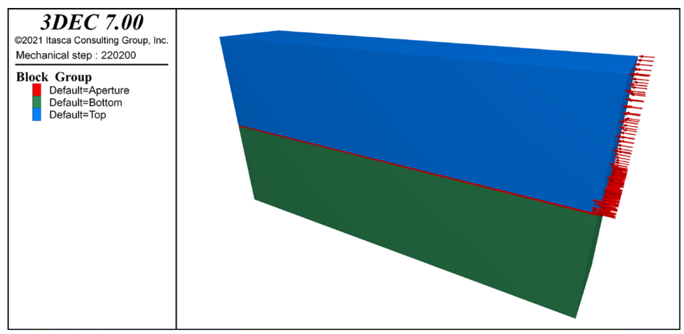

Fig. 5. Layout of the 3DEC model and applied velocity vectors (red arrows) for direct shear simulation.

3. RESULTS AND DISCUSSION

Fig. 6 and Fig. 7 illustrate the results of the direct shear test in the 3DEC model. The shear stress/displacement curves are indicated in red in the figures.

The DFNs with subhorizontal/vertical dip angles created an imbricate structure that resulted in a stepped geometry and strong shear response in the fault plane. The presence of stepped shape blocks due to the DFNs with subhorizontal/vertical dip angles drastically influences the direct shear behavior and results in an increased strength and ratio of strength development. Under direct shear, the fault plane needed to break the asperities or block before any frictional behavior was allowed or the fault plane should dilate significantly. This resulted in higher shear strength of the fault plane. On the other hand, the DFNs with oblique dip angles generated a relatively smooth surface of the fault plane. The smooth surface of the fault plane allowed deformation principally parallel to the fault plane, and only a few failures developed across the rock blocks in the model.

The higher strength of this system is due to the fact that more rock blocks in the DFNs with subhorizontal/vertical dip angles need to fail before the system is free to move. As the presence of roughness locks, the two faces of the synthetic fault and asperities need to fail (failure through rock blocks) before the synthetic fault moves under shear or needs to dilate before any movement is allowed.

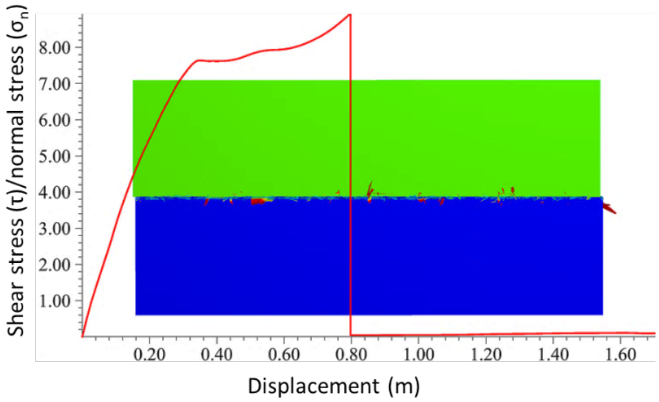

Fig. 6. Result of direct shear test considering the rough synthetic fault surface.

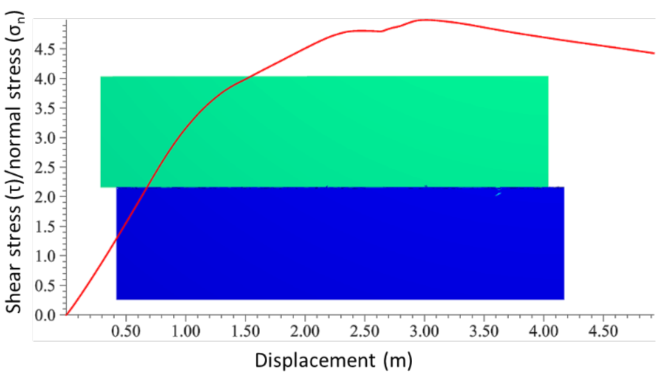

Fig. 7. Result of direct shear test considering the smooth synthetic fault surface.

Based on the 3DEC results on the direct shear test, the regression analyses were conducted to back-calculate a shear strength of the synthetic fault surface.

Fig. 8 presents the result of the regression for the rough synthetic fault surface. Fig. 9 indicates the result of the regression for the smooth synthetic fault surface.

The regression calculated for the internal friction angle was 35° for the rough synthetic fault surface and 22° for the smooth synthetic fault surface, respectively.

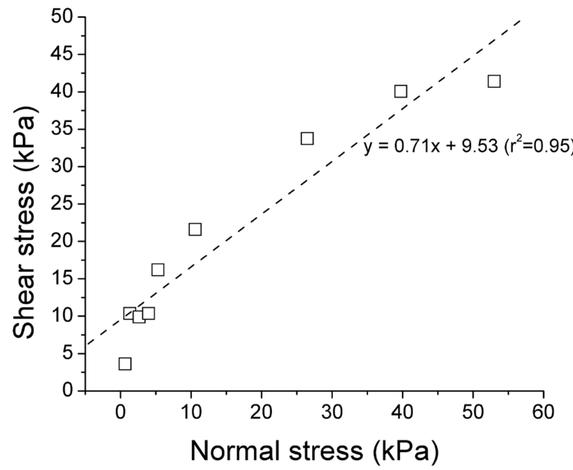

Fig. 8. Regression on the result for the rough synthetic fault surface.

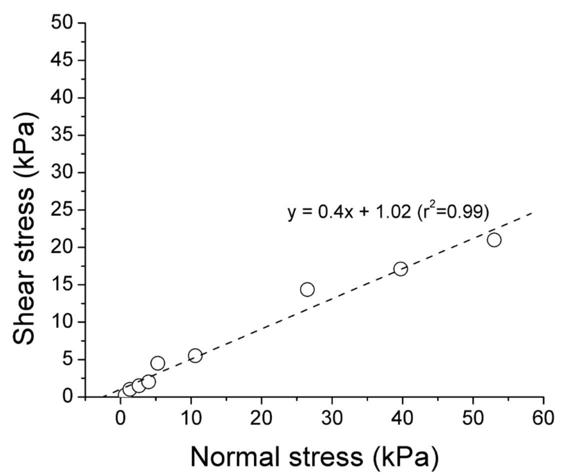

Fig. 9. Regression on the result for the smooth synthetic fault surface.

4. CONCLUSIONS

Researchers from the National Institute for Occupational Safety and Health (NIOSH) conducted a numerical simulation for the purpose of understanding the behavior of a fault associated with two different 3-dimensional geometries. 3DEC modeling in conjunction with the DFNs technique was performed to better understand the behavior of shearing faults in a relatively large-scale direct-shear test model.

This study presented the results of a series of direct-shear test simulations conducted on a relatively large scale (hundred meters). The results showed different behaviors and shear strengths for the explicitly generated 3-dimensional synthetic rock fault surface according to the orientation of the sets of DFNs. This result strongly suggests that fault surface geometric condition is one of the most important parameters to be considered for assessing bump potential associated with a fault-slip for a typical structural geologic setting. However, future studies might be performed to evaluate whether this finding holds for a mine-scale model as well as to evaluate the influences of factors affecting DFNs realization not explicitly considered in this study (such as fracture frequency) on rock fault behavior in underground excavations. A validation using experimental or field measurements might also be considered for future studies.

DISCLAIMER

The findings and conclusions in this report are those of the author(s) and do not necessarily represent the views of the National Institute for Occupational Safety and Health. Mention of any company or product does not constitute endorsement by NIOSH.

REFERENCES

1. Kim, Bo-Hyun, and Mark K. Larson (2018) Development of a fault-rupture environment in 3D: A numerical tool for examining the mechanical impact of a fault on underground excavations. *Proceedings of the 37th International Conference on Ground Control in Mining*. (Morgantown, WV: July 24–26, 2018) Englewood, CO: Society for Mining, Metallurgy, and Exploration (SME), 98–111.
2. Kim, Bo-Hyun, and Mark K. Larson (2019) Development of a 3D numerical tool for assessing the mechanical impact of a fault-rupture by normal fault on underground excavations. *Proceedings of the 53rd U.S. Rock Mechanics/Geomechanics Symposium.(New York*: June 23–26, 2019) Alexandria, VA: American Rock Mechanics Association (ARMA), 8 p.
3. MSHA (2020) Mine data retrieval system, U.S. Department of Labor, Mine Safety and Health Administration (MSHA), <https://www.msha.gov/mine-data-retrieval-system> [Accessed January 21, 2022].
4. Mauck, H. E. (1958) Coal mine bumps can be eliminated, *Mining Engineering,* Vol. 10, No. 9, 1958, p. 923.
5. Peperakis, John (1958) Mountain bumps at the Sunnyside Mines, *Mining Engineering,* Vol. 10, No. 9, 1958, pp. 982–986.
6. Agapito, Joe F. T., and Rex R. Goodrich (2000) Five stress factors conducive to bumps in Utah, USA, coal mines. *Proceedings: 19th International Conference on Ground Control in Mining*. (Morgantown, WV: August 8–10, 2000) Morgantown, WV: West Virginia University, 93–100.
7. Maleki, Hamid, and Brian White (1997) Geotechnical factors influencing violent failure in U.S. mines. *Proceedings: International Symposium on Rock Support — Applied Solutions for Underground Structures*. (Lillehammer, Norway: June 22–25, 1997) Oslo, Norway: Norwegian Society of Chartered Engineers, 1997, 208–221.
8. Boler, F. M., S. Billington, and R. K. Zipf (1997) Seismological and energy balance constraints on the mechanism of a catastrophic bump in the Book Cliffs Coal Mining District, Utah, USA, *Int. J. Rock Mech. Min. Sci.,* Vol. 34, No. 1, 1997, pp. 27–43.
9. Mark, Christopher, and Michael Gauna (2015) Evaluating the risk of coal bursts in underground coal mines. *Proceedings: 34th International Conference on Ground Control in Mining*. (Morgantown, WV: July 28–30, 2015) Morgantown, WV: West Virginia University, 47–53.
10. Rice, George S. (1936) Bumps in coal mines—theories of causes and suggested means of prevention or of minimizing effects, *Transactions of the American Institute of Mining and Metallurgical Engineers,* Vol. 119, 1936, pp. 11–39.
11. Iannacchione, Anthony T., and Joseph C. Zelanko (1995) Occurrence and remediation of coal mine bumps: A historical review, in *Proceedings: Mechanics and Mitigation of Violent Failure in Coal and Hard-Rock Mines*, ed. by Maleki, Hamid, Priscilla F. Wopat, Richard C. Repsher and Robert J. Tuchman, U.S. Department of the Interior, Bureau of Mines (USBM), pp. 27–67.
12. Chemenda, Alexandre I., Olivier Cavalié, Mathilde Vergnolle, Stéphane Bouissou, and Bertrand Delouis (2016) Numerical model of formation of a 3-D strike-slip fault system, *Comptes Rendus Geoscience,* Vol. 348, No. 1, pp. 61–69, https://dio.org/10.1016/j.crte.2015.09.008.
13. Chen, S. J., W. C. Zhu, Q. L. Yu, and X. G. Liu (2016) Characterization of Anisotropy of Joint Surface Roughness and Aperture by Variogram Approach Based on Digital Image Processing Technique, *Rock Mechanics and Rock Engineering,* Vol. 49, No. 3, pp. 855–876, 10.1007/s00603-015-0795-x.
14. Liu, Richeng, Sha Lou, Xiaojing Li, Guansheng Han, and Yujing Jiang (2020) Anisotropic surface roughness and shear behaviors of rough-walled plaster joints under constant normal load and constant normal stiffness conditions, *Journal of Rock Mechanics and Geotechnical Engineering,* Vol. 12, No. 2, pp. 338–352, https://doi.org/10.1016/j.jrmge.2019.07.007.
15. Itasca Consulting, Group, Inc., (2019) 3DEC distinct element modeling of jointed and blocky material in 3D. User's guide. version 7.0., Itasca Consulting Group, Inc., <http://docs.itascacg.com/3dec700/3dec/docproject/source/3dechome.html>.
16. Itasca Consulting, Group, Inc. (2022) Sofening-healing Mohr-Coulomb joint model, Itasca Consulting Group, Inc., <https://www.itascacg.com/software/new-joint-models> [Accessed January 26, 2022].